Cluster Compounds

Generation of Size-Controlled Pd^0 Nanoclusters inside Nanoporous Domains of Gel-Type Resins: Diverse and Convergent Evidence That Supports a Strategy of Template-Controlled Synthesis**

Benedetto Corain, Karel Jerabek,* Paolo Centomo, and Patrizia Canton**

In the realm of supported metal catalysis, the metal component is usually present as nanoparticles dispersed on the surface of suitable metal oxides[1] or on active carbon.[2] Synthetic procedures are normally directed to the generation of size-controlled metal nanoclusters, whose circumstances become mandatory when reactions to be catalyzed are "structure sensitive".[3] A paramount example of the necessity of size control is given in the area of Au^0 catalytic chemistry, specifically, the low-temperature oxidation of carbon monoxide in the presence of excess dihydrogen and the case of water gas shift reaction.[4]

In general, size control has been achieved by: directly manufacturing metal-oxide-supported catalysts;[5] by the generation of kinetically stabilized metal nanoclusters in the liquid phase[6] and subsequent transfer of the protected nanoclusters on to suitable supports;[7] by generating metal nanoclusters inside isoporous inorganic materials such as mesoporous silicas. [8]

In addition to the still-common practice of employing inorganic supports (and active carbon), a few examples of metal catalysts supported on functional resins are cited in the realm of chemical processing (such as industrial synthesis of methylisobutylketone, chemoselective hydrogenation of diolefins, acetylenes, carbonyl compounds in the presence of isobutene) and very efficient removal of dioxygen (down to the ppb levels) from industrial waters upon hydrogenation.[9] A considerable advantage of these catalysts is that they are multifunctional,[9] and may allow size control in the generation of metal nanoclusters inside polymer frameworks after the metallation–reduction steps (Figure 1).[10]

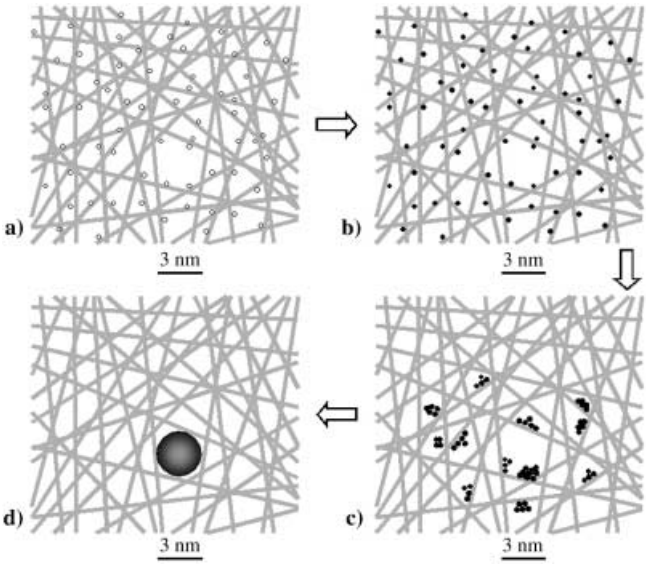

Figure 1. Model for the generation of size-controlled metal nanoparticles inside metallated resins. a) Pd^{II} is homogeneously dispersed inside the polymer framework; b) Pd^{II} is reduced to Pd^0; c) Pd^0 atoms start to aggregate in subnanoclusters; d) a single 3 nm nanocluster is formed and "blocked" inside of the largest mesh present in that "slice" of polymer framework, see text. The polymer network is drawn according to Ogston's model, reference[16].

Herein, we report on three independent, convergent pieces of structural evidence of this template-controlled synthesis strategy to obtain size-controlled metal nanoclusters suitable for synthesizing resin-supported metal catalysts. In fact, in the course of our long-standing interest in the generation and catalytic exploitation of resin-supported Pd^0 nanoclusters[9] we discovered in 1998[11] and subsequently confirmed in 2001[12] that gel-type, lightly cross-linked resins (2–8 % mol, in the absence of any porogenic agent[9]) are suitable templates for the generation of 2–4 nm Pd^0 nanoclusters. The strategy for this achievement is the dispersion of individual "Pd^{2+}" centers in the interior of the organic functional frameworks followed by their chemical reduction to Pd^0 atoms that rapidly evolve into metal nanoclusters, the size of which was tentatively expected to be controlled by the matrix nanoporosity (Figure 1). Details of the concepts outlined in Figure 1 are given in reference [12]. In this context, our previous results were encouraging,[11,12] but a quantitative confirmation of both findings and relevant rationale was lacking. We report herein on a detailed unambiguous quantitative support of the tentative conclusions of our previous papers.

[*] Prof. Dr. B. Corain
Dipartimento di Chimica Inorganica Metallorganica Analitica
Via Marzolo 1, 35131 Padova (Italy)
Fax: (+39) 049-827-5223
E-mail: benedetto.corain@unipd.it
and
Istituto di Scienze e Tecnologie Molecolari, C. N. R.
Sezione di Padova
c/o Dipartimento di Chimica Inorganica Metallorganica Analitica
Via Marzolo 1, 35131 Padova (Italy)
Fax: (+39) 049 827 5233
Dr. K. Jerabek
Institute of Chemical Process Fundamentals
Rozvojova 135, CR-16502 Suchdol, Praha 6 (Czech Republic)
E-mail: KJER@icpf.cas.cz.
Dr. P. Canton
Dipartimento di Chimica Fisica
Via Torino, 155/B, 30172 Venezia-Mestre (Italy)
Fax: (+39) 041 2346747
E-mail: cantonpa@unive.it
Dr. P. Centomo
Dipartimento di Chimica Inorganica Metallorganica Analitica
Via Marzolo 1, 35131 Padova (Italy)

[**] We are grateful to Mr. Finotto for skilled technical assistance. This work was partially supported by P.R.I.N. funding 2001–2003, Ministero dell'Università e della Ricerca Scientifica, Italy (project number 2001038991).

Supporting information for this article is available on the WWW under http://www.angewandte.org or from the author.

 DOI: 10.1002/ange.200352640

The object of our investigation is a Pd^0/resin material that we described as a chemoselective catalyst for the hydrogenation of 2-ethylanthraquinone to 2-ethylanthrahydroquinone,[13] slightly superior to the long-established commercial catalyst (Pd^0 on inorganic supports) industrially employed in a key step of the Ausimont process in the production of hydrogen peroxide. The support is a gel-type very lipophilic resin, that is polydodecylmethacrylate (92% mol)–4-vinylpyridine (4% mol)–ethylene glycol dimethacrylate (4% mol), hereafter coded as DOMA-VP.

The synthesis of Pd^0/DOMA-VP is carried out upon introducing Pd^{II} ions onto the support by using $Pd(OAc)_2$ in THF at room temperature, followed by reduction of Pd^{II} to Pd^0 in THF. The final Pd content is 1% w/w. The black material is analyzed with TEM and contains size-controlled nanoclusters (see Figure 2 and Experimental Section).

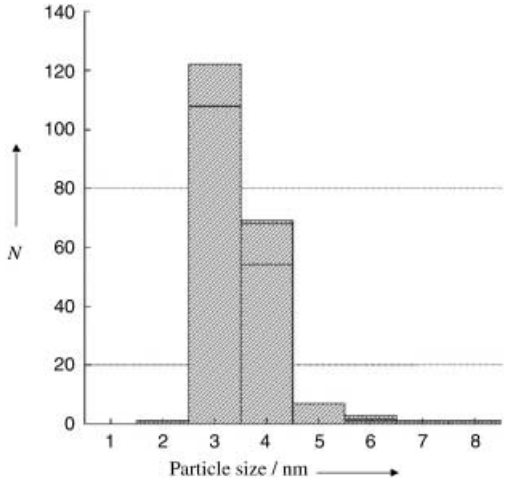

Figure 2. Size dispersion of Pd^0 nanoclusters in Pd^0/DOMA-VP. Several relevant TEM pictures are available as Supplementary Material. N = number of particles.

The surface-weighted average size [Eq.(1)]:

$$\frac{\sum_i n_i d_i^3}{\sum_i n_i d_i^2} \qquad (1)$$

obtained by TEM histogram is 3.6, in which n is the number of particles, and d is particle size.

Resin DOMA-VP was structurally investigated by ISEC (inverse steric exclusion chromatography)[14] in THF.[13] This technique provides detailed information on the nanometer-scale morphology of a given resin, after it has been swelled in a convenient liquid medium. It is based on measurements of elution behavior of standard solutes with known effective molecular sizes on a column filled with the investigated material at conditions such that the elution is influenced exclusively by the (nano)morphology of the stationary phase. As in the case of the other porosimetric methods, mathematical treatment of the elution data allows one to obtain information on the morphology of the investigated material by using a simple geometrical model. It is now established[15] that for the description of the morphology of swollen polymer gels the best tool is the so called Ogston's model,[16] which depicts pores as spaces between randomly oriented solid rods. This geometry, albeit a substantially simplified description of the morphology of swollen polymer networks, provides a fair description of both the intensive parameters (polymer chain densities) and extensive properties (specific volumes of variously dense polymer fractions). On the other hand, the conventional cylindrical-pore model commonly employed for the characterization of solid porous materials[15] relies on a geometry that is not directly related to the physical reality of the polymer framework but, from the purely mathematical point of view, it can be used to correlate the chromatographic data to the morphology of the polymer framework at the nanometer scale with essentially the same accuracy provided by Ogston's model. As a matter of fact, the porosity of a swollen gel described by using cylindrical pore geometry gives easily understandable information about the effective size of the cavities among the polymer chains, although the actual data for the specific-volume of the pores might be somewhat erroneous. However, for an investigation of the factors affecting the formation of metal nanoclusters inside the swollen polymer matrix, the effective size of the cavities used in the templating molds is much more important than their specific volume. Results of ISEC characterization of the swollen state morphology in THF of the polymer DOMA-VP are given in Table 1 and illustrated in Figure 3.

DOMA-VP has only "pores" with diameters between 2.5 and 4 nm with a clear maximum at 3.5 nm. The choice of THF

Table 1: ISEC characterization of resin DOMA-VP in THF.[a]

Pore diameter [nm]		Volume fraction [$cm^3 g^{-1}$]		Specific surface [$m^2 g^{-1}$]
	2.5	0.185	0.158	253.2
	3.0	0.927	0.791	1054.7
	3.5	1.217	1.038	1185.3
	4.0	0.637	0.544	543.7
average diameter [nm]		3.4[b]		
cumulative pore volume [$cm^3 g^{-1}$]		2.531		
cumulative surface [$m^2 g^{-1}$]		3037.9		
sum of squared errors		0.340		
number of iteration		15212		

[a] Pores from 1.0 to 2.0 nm and from 5 to 10 nm are not detected. [b] Datum calculated from Equation (1).

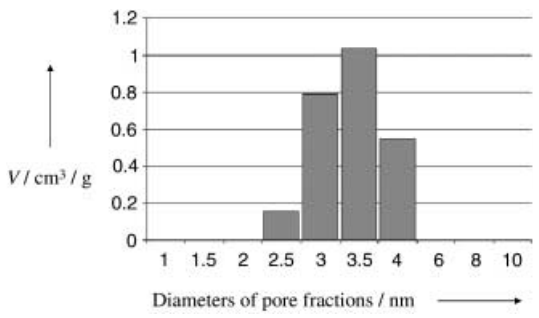

Figure 3. Nanoporosity of DOMA-VP as determined with ISEC; V = volume of the pore fractions.

as the swelling medium was dictated by the fact that the catalyst, Pd^0/DOMA-VP, could only be obtained in this solvent. From these results, one can see that the agreement between TEM evaluation of Pd^0 nanoclusters diameter and dominant pores size is almost perfect. However, we do consider this finding to be very encouraging but not conclusive.

TEM information on nanoparticle size, albeit practical and perceivable by human senses (see below), rests on the evaluation of a few hundred metal nanoclusters (if they are 3 nm in diameter, each of cluster has about 1000 Pd atoms) that is a mass of about 10^{-17} g. As we are searching for unambiguous evidence to support a general strategy of metal nanoclusters size control (TCS), it was necessary to exploit a procedure that was able to give the average nanocluster size representative of the whole specimen. In the study of supported metal catalyst the nano- and microstructural characteristics of the metal component could be determined by using X-ray-diffraction methods, which in fact are more sensitive to dimensions greater than 4–5 nm.

The determination of average particle size dimension uses Fourier coefficient analysis, which exploits the information contained in the shape and width of the XRD peak profile, corrected for the instrument contribution, to extract the average particle size and particle-size distribution.[17–19] In the case of a very dispersed catalyst, the determination of the particle size is not an easy task, as it is very difficult to establish the true background because of the large breadth of the peaks, peak overlap, and the scattering of the support. In the case in which there are very small particle sizes (less than 3 nm) the peak width is so wide that it almost disappears from the XRD pattern. This phenomenon is more striking in the case of a supported catalyst in which the scattering of the support could effectively mask the signal coming from the active phase. To take into account the signal coming from the whole active phase, that is, from particles greater than 3 nm and from particles less than 3 nm, an accurate description of the support and catalyst is mandatory. For this purpose a modified Rietveld analysis[20,21] with a physically based background, is employed in this investigation.

This method calculates the diffracted intensity of the metal phase and the background contribution due to the crystalline phase (the metal) and allows the proper scaling of the high scattering coming from the support without using any arbitrary assumption in the background description. This approach separates the scattering of the metal phase from the background, and allows the determination of the particle dimension taking into account also the contribution of sizes smaller than 2 nm. To obtain reliable results the scattering coming from the support must superimpose exactly in the region where there is no scattering contribution coming from the metal; for this reason the support and the catalyst underwent the same drying treatment by using H_2 and N_2 flux (see Experimental Section).

The sample here analyzed is a particularly difficult one as the scattering of the support peaks at a Bragg angle near to the (111) Pd reflection (see Figure 4). The Rietveld refinement is reported in Figure 4, and shows the experimental pattern, the calculated pattern, and the contribution coming

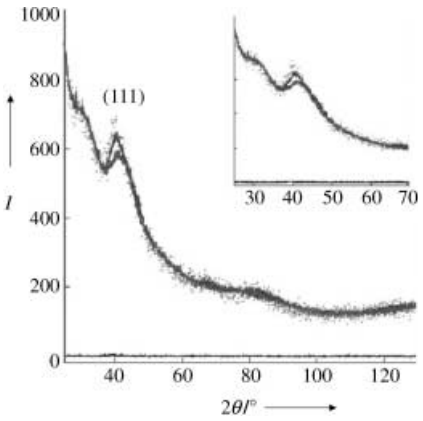

Figure 4. Rietveld refinement. In the inset the magnification of the 2θ range from 25 to 70 is reported evidencing the (111) Pd Bragg reflection. Dots are the experimental data the lower straight line is the total background the upper straight line is the calculated pattern. I = intensity (counts).

from the background. The profile parameters, obtained with Rietveld analysis, of the (111) Pd reflection, the only reflection visible in the XRD pattern, were used in the Fourier analysis; for this reason it was not possible to study the presence of strain in the sample. The procedure used to calculate the metal particle size is discussed in reference.[22]

As indicated by Guinier and other authors,[17,23] the surface weighted average sizes (defined as columns or chords in case of spherical crystallites) perpendicular to (*hkl*) planes, ⟨Ds⟩ can be obtained from the intercepts on the L axis (L being a distance in the real space) of the tangent of the size-dependent Fourier coefficients $A^S(L)$ at $L=0$ (Figure 5). By multiplying this size ⟨Ds⟩ by a factor of 3/2 the diameter of the corresponding spherical particle could be obtained, which, for this sample, is equal to 3.3(3) nm. The assumption that the particle is spherical is shown to be well justified by TEM micrographs.

Due to the importance of the determination of particle size, another independent approach was used that provides

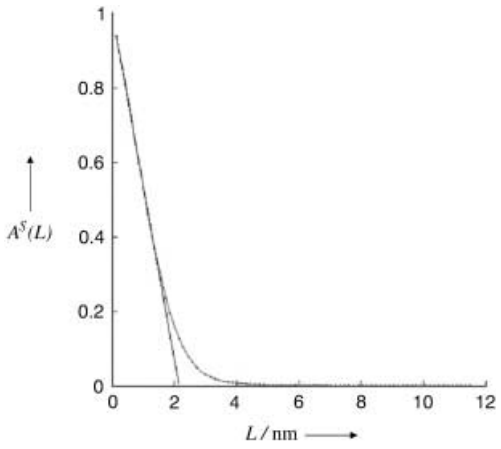

Figure 5. $A^S(L)$ Fourier transforms due to crystallite size broadening only. The intercept, with the L axis at the origin gives the surface-weighted average crystallite size.

also the number distribution function $\prod(L)$, [24] in the case of spherically shaped crystallites:

$$\prod(L) = -C\frac{\mathrm{d}}{\mathrm{d}L}\frac{\frac{\mathrm{d}^2 A^S(L)}{\mathrm{d}L^2}}{L} \quad (2)$$

in which C is a normalization constant, and the surface-averaged diameter is:

$$\langle d\rangle_S^{\mathrm{diam}} = \frac{\int_0^\infty \prod(L)\, L^3\, \mathrm{d}L)}{\int_0^\infty \prod(L)\, L^2\, \mathrm{d}L)} \quad (3)$$

the thus obtained $\langle \mathrm{d}\rangle_s$ diameter is equal to 2.6(3) nm.

In conclusion, the set of ISEC, TEM, and XRD data (Table 2) are in agreement, and provide robust evidence to support the rationale depicted in Figure 1. Intense work aimed at supporting this template-controlled-synthesis strategy for other metal centers, particularly for gold (0) is in progress.[25]

Table 2: Consistency among nanostructural features of Pd^0/DOMA-VP.

Feature	Technique	Datum	Remarks
cavities size [nm]	ISEC	3.4	–
nanocluster diameter [nm]	TEM	3.6	–
nanocluster diameter [nm]	XRD	3.3	Rietveld
nanocluster diameter [nm]	XRD	2.6	from number distribution function

Experimental Section

Catalysts Pd^0/DOMA-VP was available in the lab.[13] Solvents were of reagent grade and were used as received.

TEM analyses: JEOL 2010 with GIF, samples for TEM analysis were prepared by extensive grinding of the as-prepared material to be examined, which was subsequently ultrasonically dispersed in methanol and then transferred as a suspension to a copper grid covered with a lacey carbon film. TEM images are available in the Supporting Information.

ISEC analysis: ISEC measurements were carried out by using an established procedure and a standard chromatographic setup described elsewhere.[14,15]

XRD measurements: Philips X'Pert vertical goniometer connected to a highly stabilized generator, $Cu_{K\alpha}$ Ni-filtered radiation, a graphite monochromator, and a proportional counter with a pulse-height discriminator were used. Measurements were performed by using a sample holder that allows a gas flow[26] to avoid any contamination from air humidity, in fact both the sample and the support were extremely hygroscopic such that the water content was able to change the XRD pattern. For this reason, they were dried with a N_2 flux for 72 h. The drying process was monitored by XRD measurements by comparing the XRD patterns of each run. The corresponding diffractograms are available in the Supporting Information. The contribution due to the adsorbed water clearly affects the shape of the XRD pattern.

The sample, contained in the XRD sample holder, was subjected to a second in situ treatment with H_2 (20 mL min^{-1} 4 h) thus producing a β-PdH phase. Finally, the sample was washed with N_2 flux and monitored by XRD until β-PdH disappears and metallic Pd appears. Patterns of the sample and of the support were recorded at 295 K on a 10–140° range with a step size of 0.05° (10 s/step). For each sample seven runs were performed to have a final time of 70 s for each point. This longer period of time was used to drop the noise of data as much as possible.

Received: August 13, 2003 [Z52640]

Keywords: cluster compounds · micorporous materials · nanostructures · palladium · template synthesis

[1] For two technology-related reviews see a) E. Gallei, E. Schwab, *Catal. Today* **1999**, *51*, 535–546; b) F. Schmidt, *Appl. Catal. A* **2001**, *221*, 15–21.
[2] See for example: S. Biella, M. Rossi, *Chem. Commun.* **2003**, *3*, 378–379).
[3] a) For a classic reference see: M. Che, C. O. Bennet, *Adv. Catal.* **1989**, *36*, 54–171; b) for a recent reference see: S. Naito, M. Iwahashi, I. Kawakami, T. Miyao, *Catal. Today* **2002**, *73*, 355–361.
[4] G. Schmid, B. Corain, *Eur. J. Inorg. Chem.* **2003**, *17*, 3081–3098.
[5] S. Schimpf, M. Lucas, C. Mohr, U. Rodemerk, A. Brückner, J. Radnik, H. Hofmeister, P. Claus, *Catal. Today* **2002**, *72*, 63–78,and references therein.
[6] For an extensive review see H. Bönnemann, R. M. Richards, *Eur. J. Inorg. Chem.* **2001**, *10*, 2455–2480.
[7] C. L. Bianchi, S. Biella, A. Gervasini, L. Prati, M. Rossi *Catal. Lett.* **2003**, *85*, 91, and references therein.
[8] For two recent papers see a) Z. Konya, V. F. Puntes, I. Kiricsi, J. Zhu, J. W. Ager III, M. K. Ko, H. Frei, P. Alivisatos, G. A. Somorjai, *Chem. Mater.* **2003**, *15*, 1242–1248; b) I. Yuranov, P. Moeckli, E. Suvorova, P. Buffat, L. Kiwi-Minsker, A. Renken, *J. Mol. Catal. A* **2003**, *192*, 239–251).
[9] B. Corain, P. Centomo, S. Lora, M. Kralik, *J. Mol. Catal. A* **2003**, *204–205*, 755–762, and references therein.
[10] a) N. Toshima, Y. Shiraishi, T. Teranishi, *J. Mol. Catal. A* **2001**, *177*, 139–147b) Y. Uozumi, R. Nakao, *Angew. Chem.* **2003**, *115*, 204–207; *Angew. Chem. Int. Ed.* **2003**, *42*, 194–197.
[11] A. Biffis, A. A. D'Archivio, K. Jerabek, G. Schmid, B. Corain, *Adv. Mater.* **2000**, *12*, 1909.
[12] F. Artuso, A. A. D'Archivio, S. Lora, K. Jerabek, M. Kralik, B. Corain, *Chem. Eur. J.* **2003**, *9*, 5292–5296.
[13] A. Biffis, R. Ricoveri, S. Campestrini, M. Kralik, K. Jerabek, B. Corain, *Chem. Eur. J.* **2002**, *8*, 2962–2967.
[14] a) K. Jerábek, *Anal. Chem.* **1985**, *57*, 1595; b) K. Jerábek, *Anal. Chem.* **1985**, *57*, 1598; c) K. Jerabek, K. Setinek, *J. Polym. Sci. Part A* **1990**, *28*, 1387.
[15] "Cross Evaluation of Strategies in Size-Exclusion Chromatography": K. Jeràbek, *ACS Symp. Ser.* **1996**, *635*, 211.
[16] A. G. Ogston, *Trans. Faraday Soc.* **1958**, *54*, 1754.
[17] A. Guinier, *X-Ray Diffraction*, Freeman & Company San Francisco, **1963**, pp. 131–148.
[18] B. E. Warren, *X-Ray Diffraction*, Addison-Wesley, Reading, MA, **1969**, pp. 251–275.
[19] S. Enzo, G. Fagherazzi, A. Benedetti, S. Polizzi, *J. Appl. Crystallogr.* **1988**, *21*, 536–542.
[20] P. Riello, G. Fagherazzi, D. Clemente, P. Canton, *J. Appl. Crystallogr.* **1995**, *28*, 115- 120.
[21] G. Fagherazzi, P. Canton, P. Riello, N. Pernicone, F. Pinna, M. Battagliarin, *Langmuir* **2000**, *16*, 4539–4546.
[22] P. Canton, G. Fagherazzi, M. Battagliarin, F. Menegazzo, F. Pinna, N. Pernicone. *Langmuir* **2002**, *18*, 6530–6535.
[23] R. J. Matyi, L. H. Schwartz, J. B. Butt, *Catal. Rev. Sci. Eng.* **1987**, *29*, 41–99.
[24] S. Ciccariello, G. Fagherazzi, A. Benedetti, *Acta Crystallogr. Sect. A* **1990**, *46*, 187–194.
[25] B. Corain, C. Burato, P. Centomo, S. Lora, W. Meyer-Zaika, G. Schmid, contribution to GOLD2003, Vancouver, **2003**; submitted to *Gold Bull.*
[26] P. Canton, P. Riello, A. Furlan, A. Minesso, L. Bertoldo, F. Pinna, A. Benedetti, *Catal. Lett.* **2000**, *69*, 17–20.

